EEET ECOLOGICAL ENGINEERING & ENVIRONMENTAL TECHNOLOGY

Ecological Engineering & Environmental Technology, 2025, 26(2), 66–85
https://doi.org/10.12912/27197050/196519
ISSN 2719–7050, License CC-BY 4.0

Received: 2024.11.19
Accepted: 2024.12.20
Published: 2025.01.01

Mapping forest fire risk: A comprehensive approach using analytical hierarchy process, geographic information system, and remote sensing integration

Reem Salman[1], Ali Karouni[2], Nizar Hamadeh[2*], Elias Rachid[3]

[1] Lebanese University, EDST, Lebanon, Beirut, Lebanon
[2] Lebanese University, Faculty of Technology, Saida, Lebanon,
[3] Saint-Joseph University, Ecole Supérieure D'ingénieurs de Beyrouth, Beirut, Lebanon
* Corresponding author's e-mail: nizar.hemadeh@ul.edu.lb

ABSTRACT

Wildfire is one of the natural hazards that is escalating globally. While it can cause extensive harm worldwide, significant economic losses, infrastructural damage, and severe social disruption worldwide, the Mediterranean region is vulnerable because of its distinct climate and vegetation patterns. This study uses geospatial technologies and the multi-criteria decision-making method with Analytical Hierarchy Process to assess and map wildfire risk, using different factors like anthropogenic, meteorological and topographic data. The resulting fire risk map categorizes the area into five zones: very high, high, moderate, low, and very low risk. Findings indicate that 34.89% of the area is at moderate risk, 33.45% at high risk, and 7.62% at very high risk. The model's final susceptibility map was found to be consistent with the historical fire events that occurred in the area of study, demonstrating the efficacy of the approach utilized to identify and map fire risk zones. This model will enhance disaster response capabilities and preparedness through coordination with stakeholders and development of sustainable forest management contingency plans for more resilient communities.

Keywords: remote sensing, GIS, wildfire, risk mitigation, MCDM.

INTRODUCTION

The combined impact of global climate change and human activities is leading to a troubling decrease in forest areas, with uncontrollable forest fires playing a significant role in this ongoing decline. Uncontrolled forest fires are a major contributor to the rapid degradation of global forest ecosystems, as highlighted by Venkatesh et al. (2020). These fires pose a severe threat, especially in rural regions, where they lead to the destruction of life and property and cause considerable harm to the local ecological balance. The world is experiencing an exceptional moment of fragility and uncertainty, and climate-fueled disasters are becoming more frequent and intense. In Mediterranean countries, wildfires pose a significant risk with both high probability and severe impact. Wildfire is one of the primary shaping factors of Mediterranean ecosystems (Paula et al., 2009), having an annual impact between 700.000–1 million hectares on Mediterranean forests globally (Dimitrakopoulos and Mitsopoulos, 2006). The Mediterranean Basin is particularly vulnerable to fires, primarily due to the abandonment of agricultural lands. This has led to the growth of early-successional plant species that are highly flammable and accumulate significant amounts of dead biomass. This buildup of dry material increases the likelihood of fires starting and spreading (Santana et al., 2018).

The Mediterranean region stands out as the globe's third richest biodiversity hotspot (Mittermeier et al. 2004). Throughout history, numerous civilizations have depended on its forest resources for a variety of purposes, including cultural,

economic, social, and aesthetic services. These fires not only threaten biodiversity but also impact the livelihoods of local communities and the stability of ecosystems. The increasing frequency and intensity of these fires can be attributed to factors such as climate change, land-use changes, and inadequate forest management practices, have significantly contributed to the rise of wildfires with anthropogenic factors. Several environmental and socioeconomic elements have been impacted by these changes.

Despite regional trends, research on fire events in the Eastern and Southern Mediterranean Basin is still limited, lacking systematic and unified documentation (Belhadj-Khedher et al., 2018; Aini et al., 2019). Conversely, changes in fire suppression strategies in parts of the European Mediterranean, such as France since the 1990s and Spain, Italy, and Portugal since the 2000s, have led to a decrease in fire incidents in the mentioned regions (Ruffault and Mouillot, 2015). However, Mediterranean-wide analyses still depend on national databases to forecast future fire risks across the region (Ruffault et al., 2020). To effectively study wildfires, a fundamental prerequisite would be defining and measuring their key components, such as frequency, intensity, type, and seasonality across the different regions of the Mediterranean Basin (Gill, 1975).

In the Eastern Mediterranean Basin, existing data are often non-uniform and of low accuracy (Faour, 2004) (FAour, 2015). A clear and comprehensive forecasting solution or dashboard that shows the interrelation between the spatial representation of wildfire in this area and fire response management is lacking. This gap prevents the assessment of future threats to forest sustainability, influenced by climate change and other contributing factors (Majdalani et al., 2022).

Lebanon has been facing increasing concerns of forest fires which mainly are of natural or man-made origin. As a Mediterranean country, Lebanon is highly susceptible to forest fires during the summer, as the weather gets warm and dry, and the vegetation is highly flammable (World Bank, 2011). The country's socio-political and economic situation has impaired progress in risk management leading to insufficient forest management and response capacities.

Lebanon has been experiencing an increase in forest fires throughout the years. Within the last 22 years (2001–2023) the country has lost 1.83 thousand hectares of tree cover due to fires (Global Forest Watch, 2024). From July 24, 2023, to July 29, 2024, VIIRS (Visible Infrared Imaging Radiometer Suite) reported 42 high-confidence fire alerts, marking a significant increase compared to the number of alerts recorded in previous years since 2012 (Global Forest Watch, 2024).

Lebanon is anticipated to face an increase in temperature, more frequent and severe droughts, and reduced precipitation. Studies predict that the average increase in temperature will be of 1 °C to 2 °C by 2040 on the coast and 2 °C to 5 °C by 2090 inland, compared to the baseline of years 1991 to 2020 baseline (Ministry of Environment, Lebanon, "Vulnerability and Adaptation").

Lebanon's 139.000 hectares of forests plays a crucial role for various ecosystem services to both local communities and the country. Estimating the exact value of these services is complex, but World Bank research estimates that Lebanon loses about $296 per hectare in economic value each time a forest fire occurs (PreventionWeb, 2022). As climate change is exacerbating the risks of wildfire, Lebanon should rapidly ensure sustainable forest management, and enhance fire detection capacities and prevention efforts.

No such methodology prior to the present study has been explored for mapping fire risk zones in the study area. Tentative maps indicating fire risk have been developed for Lebanon (Faour, 2004) (Faour et al., 2006) (Masri et al., 2003). Nevertheless, these maps often fall short of accurately reflecting the seasonal timing of fires, the total area burned (mapping), and the precise locations of fire boundaries.

Understanding and predicting wildfires is challenging, yet significant technological advances have improved monitoring and modeling capabilities. These advancements have led to a data-driven approach to wildfire modeling, and there is growing interest in applying machine learning techniques to wildfire science and management (Jain er al., 2020). Geographic information system (GIS) technology has been essential for creating forest fire susceptibility maps by effectively processing and integrating geospatial data (El Hafyani et al., 2020) (Teodoro and Duarte, 2013). Moreover, using remote sensing and satellite images has become essential for collecting the data needed to create these maps (Mohajane et al., 2021). GIS technologies provide a fast, economical, and efficient way to obtain the necessary information for forest fire risk assessment. By leveraging GIS and integration of

machine learning, authorities can better predict fire-prone areas, enhance early warning systems, and implement effective fire management strategies to mitigate the impact of forest fires (Bui et al., 2018). Technological advancements have enhanced the efficiency of wildfire detection methods by integrating machine learning techniques with GIS and remote sensing to assess fire risk (Ghali et al., 2020).

Various studies have explored the integration of these systems, with some employing pairwise comparisons to assign weights based on expert judgments or existing literature (Mazzeo et al., 2022). A similar approach for weight assignment was employed by Mazzeo (Mazzeo et al., 2022) in Italy using Multi-Criteria Decision Support, and Lamat (Lamat et al., 2021) in India using MCDM with analytical hierarchy process (AHP) to compare the parameters. Additionally, Majlingová (Majlingová, 2015) in Slovakia used Multi-Criteria Decision Analysis, and Pourghasemi (Pourghasemi et al., 2016) in Golestan Province, Iran used Mamdani fuzzy logic (MFL) and modified-AHP models. Abdo et al. (2022) conducted a study to assess and compare the effectiveness of the frequency ratio (FR) and AHP methods for mapping forest fire vulnerability in the Al-Draikich region of western Syria.

AIM OF THE STUDY

This study focuses on creating a forest fire risk map for Lebanon by combining satellite imagery, topographic data, and additional information through GIS technology. Furthermore, we introduce a methodology that leverages remote sensing, GIS techniques, and machine learning to fill existing gaps in wildfire research for Lebanon. The AHP, a widely used multi-criteria decision-making technique, will be employed to develop the Forest Fire Risk Map (Triantaphyllou and Triantaphyllou, 2000). Various data types – including weather, topography, and human activities – will be collected. Nine factors (elevation, slope, aspect, proximity to urban areas, agriculture, roads, temperature, wind speed, and land use/land cover) will be analyzed in ArcGIS Pro, using data gathered from various accessible sources.

This map will assist emergency response teams, environmental organizations, local authorities, disaster risk management committees, and other governmental bodies in preventing or reducing fire risks in forests. It will also support timely interventions when fires occur and aid in proactive measures to mitigate fire risk.

AREA OF STUDY

The study area extends along the eastern Mediterranean coastline, characterized by mountain ranges exceeding 2.500 meters in height and covering an area of 10.452 km² (Bugh et al., 2024) Mediterranean coastline, characterized by mountain ranges exceeding 2.500 meters in height and covering an area of 10.452 km² (Bugh et al., 2024). Lebanon is structured into eight governorates – Beyrouth, Mount Lebanon, Bekaa, North, South, Nabatiyeh, Aakkar, and Baalbak El-Hermel – and further segmented into districts (qadaa or caza) (Bugh et al., 2024).

Lebanon's terrain consists of 4 notable regions which are: a narrow coastal plain hugging the Mediterranean Sea, the impressive Lebanon Mountains, the verdant Bekaa Valley, and the Anti-Lebanon and Mount Hermon mountain ranges that run alongside the Lebanon Mountains. In addition, Lebanon was once rich in forests, however, centuries of grazing, burning, and logging have severely limited the regeneration of this natural vegetation Lebanon falls within the Mediterranean climate zone (Csa) (Figure 1), known for its hot, dry summers and mild, wet winters, which is typical of Mediterranean climates (World Bank, 2023). The average temperature throughout the year is approximately 15 degrees Celsius. Rainfall varies from 700 to 1.000 millimeters along the coast and can reach up to 1.600 millimeters in the mountainous regions, where precipitation includes both rain and snow (World Bank, 2022a).

According to the 2017 land cover/land use map (CNRS, 2017), Mount Lebanon, Baalbek-Hermel, and North are the governorates with the most extensive areas of forest and shrubland, covering 80.100 hectares, 71.500 hectares, and 40.200 hectares, respectively. They are followed by Nabatiyeh (29.300 hectares), South (28.800 hectares), Beqaa (28.300 hectares), and Akkar (27.200 hectares) (CNRS, 2–17). The governorate of Beirut is fully designated as urban land area (103 hectares) of forests, shrublands, and grasslands by Governorate in Lebanon and their percentage coverage – based on data from

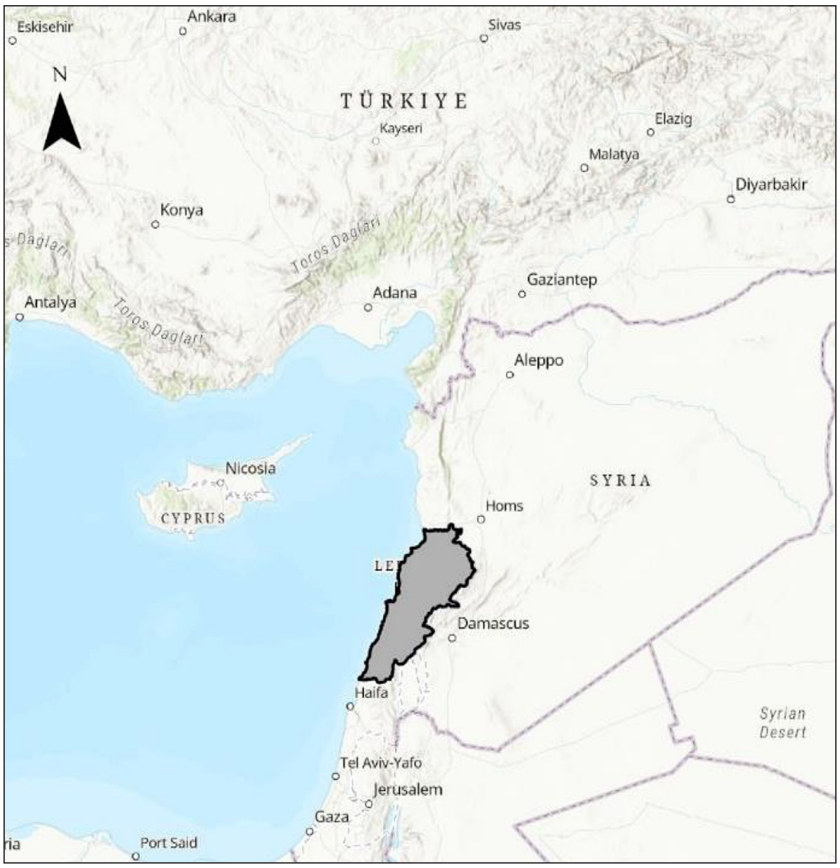

Figure 1. Location of Lebanon within the Mediterranean basin

Table 1. Area (103 hectares) of forests, shrublands, and grasslands by governorate in Lebanon and their percentage coverage – based on data from CNRS (2022)

Parameter	Akkar	Baalbek - Hermel	Beqaa	Mount-Lebanon	Nabatiyeh	North	South
Total area (10^3 ha)	79.0	285.3	141.3	197.3	110.0	118.7	92.4
Forests and shrubs (10^3 ha)	27.2	71.5	28.3	80.1	29.3	40.2	28.8
Forests and shrubs (%)	34.4	25.0	20.0	40.6	26.6	33.9	31.1
Grass (10^3 ha)	2.9	2.7	6.2	9.4	11.4	3.5	6.1
Grass (%)	3.6	0.9	4.3	4.7	10.3	2.9	6.6

CNRS (2027) (Table1). Lebanon's diverse topography and climate create a range of bioclimatic zones. Forests and wooded areas cover approximately 23% of the country, supporting a rich biodiversity. Lebanon is rich in plant diversity, hosting approximately 2600 species of terrestrial plants, which account for 1.11% of all plant species worldwide. In addition, 8.5% of these species are unique to Lebanon, Syria and Palestine with 3.5% found exclusively in Lebanon. What stands out is Lebanon's extraordinary floral density that it ranks among the highest in the Mediterranean Basin, with about 0.25% plant species per square kilometer Lebanon's socioeconomic challenges are expected to worsen due to climate change, which will heighten the country's long-term vulnerabilities. Projections from Lebanon's fourth national communication to the UN Framework Convention on Climate Change (UNFCCC) indicate that by 2040, temperatures could rise by 1 °C along the coast and 2 °C inland, with a potential decrease in rainfall of 10 to 20% (World Bank, 2023). These climatic shifts, including more frequent extreme weather events, are anticipated to create significant difficulties for managing water resources and will impact critical areas such as agriculture and forestry (World Bank, 2023).

MATERIALS AND METHODS

Methodology

In this research, AHP, a widely used multi-criteria decision-making technique (Triantaphyllou and Triantaphyllou, 2000) was applied to identify and map regions at high risk of fire in Lebanon by developing a forest fire risk map.

By integrating GIS technology with AHP and remote sensing through satellite images, the study analyzed nine key factors contributing to fire risk. Different data sets sources were utilized to support the identification and mapping process, ensuring a comprehensive assessment of fire susceptibility across the region. However, the overall methodology of the study is presented in Figure 4.

Resources and data preparation

Active fire data – NASA FIRMS

Because the lack of detailed of fire records in Lebanon NASA's Fire Information for Resource Management System (FIRMS) was relied upon to determine the dates and locations of fires. FIRMS is a widely recognized tool for identifying fire perimeters in global burnt area mapping algorithms by using the remote sensing techniques (Pinto et al., 2021).

The system offers near real-time data on active fire locations which is based on observations captured by NASA's moderate resolution imaging spectroradiometer (MODIS) (NASA FIRMS, n.d.). Since the year 2000, MODIS has provided precise information about active fires or thermal hotspots by identifying the center of a 1 km pixel where fire activity has been detected by its algorithm (Giglio et al., 2016). However, the number of recorded fire events is lower than the actual occurrences in Lebanon over the last 20 years. This data remains our only available source, even though hotspots can still miss some smaller fires. However, a new approach was developed: a dashboard that aggregates all fire related news posted by the Lebanese Civil Defense and the Lebanese Red Cross. This dashboard, that has been operational since April 2024, automatically updates and maps all fire events reported to accurately map the fires and the burned areas (Figure 2).

Landsat data processing

Fire contours over Lebanon's wildland areas were created using Landsat 7 (ETM+) and Landsat 8 (OLI) data from 2000 to 2015, as well as Sentinel-2 (MSI) data from 2016 to 2020. This processing was conducted with the assistance of Google Earth Engine (GEE), which served as a semi-automated tool for detecting burnt areas. Landsat 9 was utilized for mapping recent fire events on the dashboard related to the Lebanese Red Cross.

Now a day the most usable tool computes two key spectral indices are: the normalized difference vegetation index (NDVI) (Rouse et al., 1973), this is used to evaluate plant health, and the normalized burn ratio (NBR) (Key and Benson, 1999),

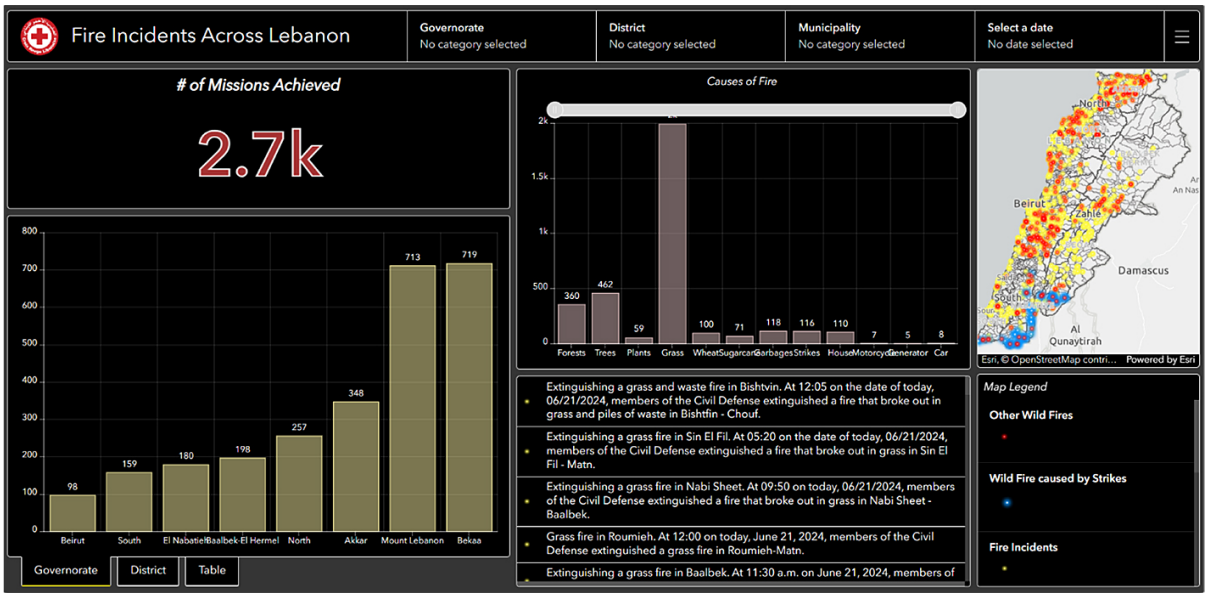

Figure 2. Fire incidents across Lebanon dashboard

which helps to measure the severity of burns. To establish the pre- and post-burn periods, users need to specify the burn date and select the target area. These indices are represented using an RGB color scale. Users then classify areas as either burnt or unburnt to train a random forest classifier, which uses supervised classification to detect changes in the NDVI and NBR composites.

Each fire is initially located using NASA's FIRMS, to identify a processing zone. The resulting fire polygons are visually interpreted and manually refined to achieve the desired visual accuracy (Figure 3). This process involves removing commission errors (such as fire polygons detected in agricultural lands) and reprocessing omitted burned areas by expanding and multiplying the training zones. While this procedure is time-consuming, it ensures a level of visual validation that automated methods typically cannot provide.

Metrological data

The Weatherbit API was utilized to collect meteorological data due to gaps identified in the climatic information from various weather stations across Lebanon. The Weatherbit API delivers real-time weather data for any location worldwide, sourced from over 47.000 active weather stations, as well as Doppler radar and meso-reanalysis data. It provides current weather conditions from a network of sub-hourly reporting stations and includes atmospheric meso-analyses.

This API offers a real time weather updates from a network stations which report several times an hour. Each request gives us the most recent and nearest weather data, along with detailed atmospheric analysis (Weatherbit, n.d.). To make a weather map for Lebanon, it is essential to generate a fixed location as a cell grid. Then, a script runs and requests from each API for each location (Grid Cell) the weather data and stores the data in the feature class which is used to create a raster for each weather information. The Weather bit API was preferred as a selection because it is more accurate and complete, with no missing data compared to other options. Despite being a paid service, it offers superior results of weather data.

Digital elevation model

This study utilized elevation, aspect and slope data from the advanced spaceborne thermal emission and reflection radiometer (ASTER) Global digital elevation model (GDEM). Produced by the ASTER instrument on the Terra satellite, this high-resolution dataset provides highly detailed and accurate elevation information with a spatial resolution of 30 meters maximum. Its precision makes it an essential resource for geospatial analysis (NASA, n.d.). The ASTER GDEM data is publicly available and can be accessed through NASA's Earthdata platform. This dataset covers the entire globe, offering consistent and comprehensive elevation information crucial for various environmental and scientific applications. By integrating ASTER GDEM data into GIS software, it is possible to derive essential topographic parameters such as elevation, slope, and aspect, which are critical for modeling and analyzing wildfire risks and other geospatial phenomena. However, the overall methodology of the present study is shown in the Figure 4.

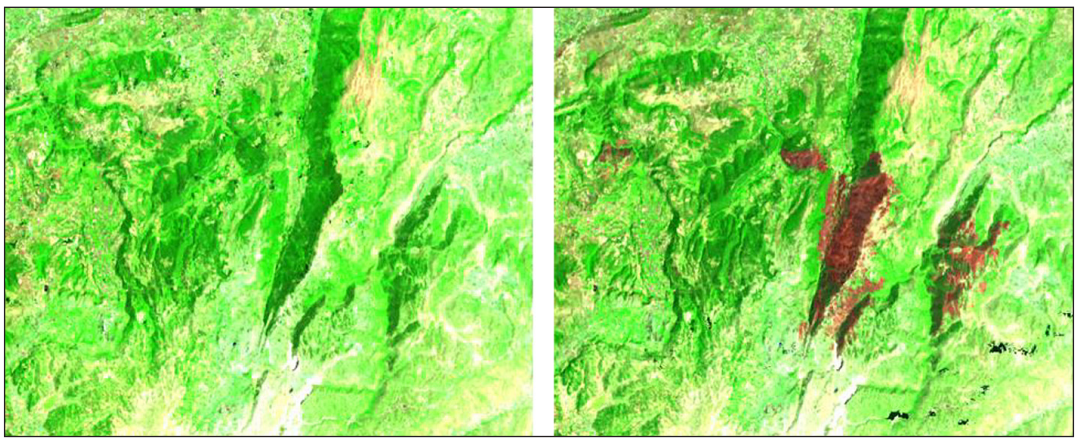

Figure 3. Pre- and post-fires in Akroum (Akkar) in 29-7-2022

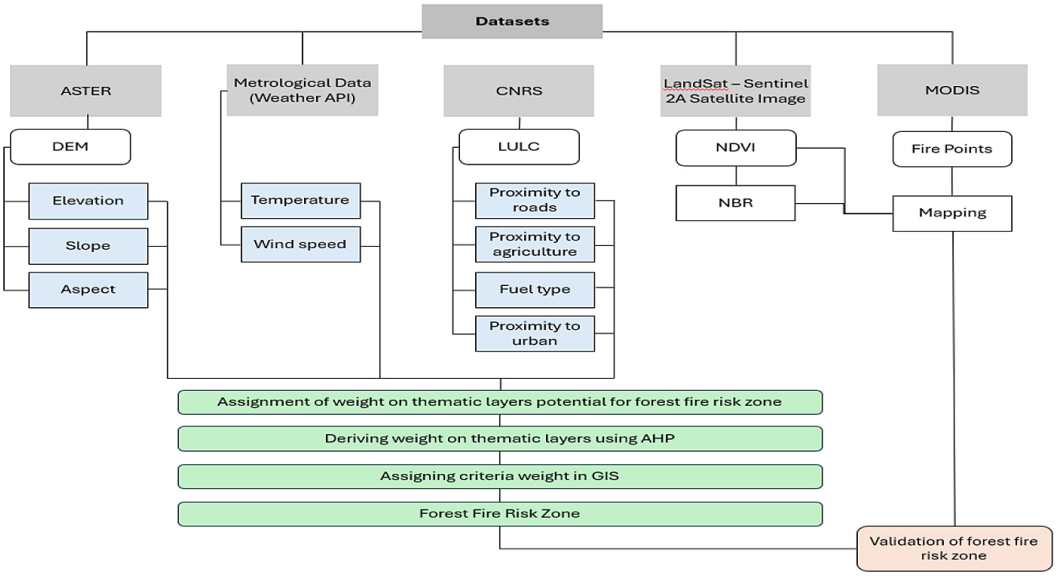

Figure 4. Flowchart of the methodology

INFLUENTIAL FACTORS

Topography

Slope

Slope (°) measures the rate of change in elevation and is typically expressed as the angle or gradient of the terrain's surface. Fires often spread more rapidly uphill because the vegetation is pre-heated and the flames have more direct contact with the surface. In fact, a fire's speed can double with each 10-degree increase in slope, as the slope enhances the effect of the wind by directing the flames and pre-heating the vegetation.

Aspect

Aspect (°) denotes the direction of the greatest change in elevation between each cell and its adjacent cells, with measurements given in degrees from north (0° for north, 90° for east, 180° for south, and 270° for west) (Esri, n.d.). In the northern hemisphere, north-facing slopes are typically shaded, while south-facing slopes receive more solar radiation because they are oriented towards the sun and are not directly shaded by surrounding terrain. The direction a slope faces influences fire behavior in various ways. South- and west-facing slopes, which receive more direct sunlight throughout the day, particularly in summer, tend to have drier soil and vegetation due to higher rates of evapotranspiration compared to north- and east-facing slopes. West-facing slopes are warmer in the late afternoon and evening due to direct sunlight, while east-facing slopes warm up quickly in the morning after cooler nights.

Elevation

Elevation (m), or the height above sea level (m a.s.l.), significantly influences wildfire behavior and risk. In the context of Lebanon's diverse topography, which includes coastal plains, hilly areas, and mountain ranges, elevation interacts with other factors such as temperature, humidity, and vegetation types. Forest fires typically decrease with rising elevation, as cooler temperatures and higher humidity at higher altitudes contrast with the conditions at lower elevations (Rothermel, 1983).

Metrological data

Temperature

As temperatures (°C) increase throughout the day, the air can hold more moisture which causes relative humidity to decrease. This means the air has low moisture compared to its maximum capacity. During the night cooler air holds more moisture and fuels soak up this moisture from the damp environment which reduce fire activity.

Wind speed

Wind speed (m/s) significantly impacts the intensity and spread of a fire in an area. Stronger

winds accelerate fire spread by supplying additional oxygen, which intensifies the flames and preheats and dries the fuel in front of the fire. Winds can carry sparks and embers ahead of the main blaze, leading to spot fires. Additionally, wind moving up slopes can increase the fire's spread, while draws and ravines can channel flames upward like chimneys.

Land use and land cover (LULC)

Fuel types

Human activities greatly expedite changes in LULC, resulting in considerable effects on forests and ecosystems (Agarwal, 2002; Kumar et al., 2018). Previous studies have highlighted the crucial role of land cover classifications in assessing fire risk, given their relationship with different fuel types and their characteristics (Vadrevu et al., 2010) (Szpakowski and Jensen, 2019).

Proximity to urban

Areas adjacent to urban areas are more likely to experience fires than area regions situated further from these lands. Urban areas often contribute to fire risk through human activities such as improper disposal of flammable materials, construction work, and increased heat from buildings and infrastructure. As the distance from urban areas grows, the influence of these activities diminishes, leading to a reduced risk of fire (Raval and Motiani, 2022).

Proximity to agriculture

Areas adjacent to agricultural lands are more likely to experience fires than areas situated further from these lands. This is because agricultural activities often involve the use of machinery, burning of crop residues, and other practices that can increase the likelihood of fire ignition. As the distance from agricultural lands increases, the influence of these activities diminishes, leading to a lower fire risk (Glagolev et al., 2018).

Proximity to roads

Areas adjacent to roads are more likely to experience fires than areas situated further from these roads. Roads are often associated with human activities that can increase fire risk, such as vehicle emissions, discarded cigarettes, and roadside vegetation management. As the distance from roads increases, the influence of these factors diminishes, leading to a lower fire risk (Raval and Motiani, 2022).

METHODS

GIS integration and raster calculation for fire risk mapping

The study utilized the integration of GIS-based multi-criteria decision-making (MCDM) and the AHP to identify and map areas within the study region that are potentially vulnerable to fire. This approach involved using spatial data layers corresponding to nine factors (elevation, slope, aspect, proximity to urban, fuel types, proximity to agriculture, proximity to agriculture, temperature, and wind speed) were processed using GIS and remote sensing techniques to create spatial data layers in raster format. (Fig. the parameters diagram).

The raster factor maps were standardized to a uniform scale ranging from 1 (very low) to 5 (very high) using the reclassify tool in the spatial analyst tools. The raster factors were then resampled to a 10 meters resolution using the resample tool within ArcGIS's data management tools. In addition, the agricultural and forest cover rates were assessed based on the guidelines set in the Lebanese National Action Plan (NAP) of 2003. After reclassifying the maps of all fire-controlling factors, each factor was assigned a relative weight using the AHP model. The final national fire susceptibility map was then produced by overlaying the nine fire-controlling spatial layers using the raster calculator tool in the ArcGIS environment. The AHP analysis, along with the processing, generation, and overlaying of digital raster layers, was conducted utilizing ArcGIS, Jupyter Lab, and Microsoft Excel.

Analytical hierarchy process (AHP)

The AHP introduced by Saaty (1987), is widely utilized to assess and assign relative importance to different criteria in studies. While several methodologies, including fuzzy sets (Bellman and Zadeh, 1970), linguistic variables (Chen and Hwang, 1992), and AHP (Saaty, 1987), are applied for determining fire risk zones, AHP remains the most prevalent method (Sharma et al., 2014; Vadrevu et al., 2010). In this study, AHP was used to assign weights to various factors influencing fire susceptibility, following Saaty's step-by-step procedure.

The AHP was applied to identify and map fire-prone areas in Lebanon by developing a forest fire risk map. This study combined GIS technology with AHP to assess nine critical factors influencing fire risk. Multiple spatial criteria (such as aspect, slope, distance to the road, etc.) must be combined under suitable conditions to determine the likelihood of fire ignition and spread in forest areas. GIS is highly effective for simultaneously analyzing multiple spatial criteria and drawing effective conclusions (Key and Benson, 1999). These factors were evaluated based on their relative importance, categorized into levels such as very low, low, moderate, high, and very high. The procedure is implemented as follows:

To create the pairwise comparison matrix as seen in Table 2. Each factor was assigned a value ranging from 1 to 9 to represent its relative importance. The value 1 means that the two factors are equally important, while the value 9 means that one factor is significantly more important than the other.Applying the formula, sum the values in each column of the pairwise comparison matrix. (Table 3) (Equation 1):

$$Lij = \sum_{n=1}^{n} Cij \quad (1)$$

where: *Lij* – total column value of the pair-wise comparison matrix; *Cij* – the analysis's criteria that were applied.

Table 2. Scale of a pair wise comparison

Intensity importance	Linguistic variables
1	Equal importance
2	Equal to moderate importance
3	Moderate importance
4	Moderate to the strong importance
5	Strong importance
6	Strong to the very strong importance
7	Very strong importance
8	Very to the extremely strong importance
9	Severe importance

Table 3. Distribution of fire susceptibility per area in Lebanon

Fire susceptibility	Area (ha)	Area (%)
Very low (1)	39.650	4.5
Low (2)	172.425	19.54
Moderate (3)	307.950	34.89
High (4)	295.225	33.45
Very high (5)	67.275	7.62

To create a normalized pair-wise comparison matrix, divide each matrix element by the total number of rows in the matrix (Table 4) (Equation 2):

$$Xij = \frac{Cij}{Lj} \quad (2)$$

where: *Xij* – normalized pair-wise comparison matrix.

Calculate the standard weight by dividing the sum of the normalized rows of the matrix by the total number of criteria/parameters (N) using the following formula. (Equation 3):

$$Wij = \frac{\sum_{j=1}^{n} Xij}{N} \quad (3)$$

where: *Wij* – standard weight.

The following formula was used to calculate the consistency vector values (Equation 4):

$$\lambda = \sum_{i=1}^{n} CVij \quad (4)$$

where: λ – consistency vector.

After knowing the weights for each fire-controlling factor, a consistency check was carried out to ensure the comparisons if they accurate and reliable. This involved calculating the consistency index (*CI*) using Equation 5 by following the method outlined by Saaty (1987).

$$CI = \frac{\lambda max - n}{n-1} \quad (5)$$

The consistency ratio (CR) is calculated using the following formula (Equation 6):

$$CR = \frac{CI}{RI} \quad (6)$$

where: *RI* – random inconsistency, which varies depending on the number of factors used in the pairwise comparison matrix Tables 5–7).

If and only if the CR is 0.10 or greater this indicates that the comparisons lack sufficient consistency, requiring the process to be revisited and adjusted until the CR falls below the 0.10 of the thresholds (Saaty, 1987).

Method of wildfire susceptibility map preparation

To create the fire susceptibility map for the study area, spatial layers were combined using Equation 7 through raster calculator in ArcGIS's spatial analyst extension. For each factor influencing fire risk was carefully prepared

Table 4. Pair-wise comparison matrix

Factors	FT	EL	SL	AS	TEMP	WS	PTR	PTA	PTU
FT	1	3	3	2	1	1	3	2	3
EL	1/3	1	2	1	1	1	3	3	4
SL	1/3	1/2	1	3	1	1	1	3	1
AS	1/2	1	1/3	1	1	1	2	1	2
TEMP	1	1	1	1	1	1	1	1	1
WS	1	1	1	1	1	1	1	1	1
PTR	1/3	1/3	1	1/2	1	1	1	5	7
PTA	1/2	1/3	1/3	1	1	1	1/5	1	4
PTU	1/3	1/4	1	1/2	1	1	1/7	1/4	1

Note: FT fuel type, EL elevation, SL slope, AS aspect, TEMP temperature, WS wind speed, PTR proximity to road, PTA proximity to agriculture, PTU proximity to urban area.

Table 5. Normalized Pair-wise Comparison Matrix

Para-meter	FT	EL	SL	AS	TEMP	WS	PTR	PTA	PTU	Sum	CW	CW(%)
FT	0.1875	0.35646	0.28125	0.181818	0.111111	0.111111	0.243056	0.115942	0.125	1.713224	0.190358181	19.04
EL	0.0625	0.118812	0.1875	0.090909	0.111111	0.111111	0.243056	0.173913	0.166667	1.265578	0.140619829	14.06
SL	0.0625	0.059406	0.09375	0.272727	0.111111	0.111111	0.081019	0.173913	0.041667	1.007204	0.111911518	11.19
AS	0.09375	0.118812	0.03125	0.090909	0.111111	0.111111	0.162037	0.057971	0.083333	0.860285	0.095587175	9.56
TEMP	0.1875	0.118812	0.09375	0.090909	0.111111	0.111111	0.081019	0.057971	0.041667	0.893849	0.099316599	9.93
WS	0.1875	0.118812	0.09375	0.090909	0.111111	0.111111	0.081019	0.057971	0.041667	0.893849	0.099316599	9.93
PTR	0.0625	0.039604	0.09375	0.045455	0.111111	0.111111	0.081019	0.289855	0.291667	1.126071	0.125118998	12.51
PTA	0.09375	0.039604	0.03125	0.090909	0.111111	0.111111	0.016204	0.057971	0.166667	0.718577	0.079841851	7.98
PTU	0.0625	0.029703	0.09375	0.045455	0.111111	0.111111	0.011574	0.014493	0.041667	0.521363	0.057929248	5.79

Note: FT fuel type, EL elevation, SL slope, AS aspect, TEMP temperature, WS wind speed, PTR proximity to road, PTA proximity to agriculture, PTU proximity to urban area, CW criteria weights.

Table 6. Calculating consistency

Para-meter	FT	EL	SL	AS	TEMP	WS	PTR	PTA	PTU	WSV	CW	WSV/CW
FT	0.190358	0.421859	0.3357	0.191174	0.0993166	0.099317	0.375356995	0.159683702	0.173787744	2.046588214	0.190358181	10.75124904
EL	0.063453	0.14062	0.2238	0.095587	0.0993166	0.099317	0.375356995	0.239525553	0.231716992	1.568715507	0.140619829	11.15572049
SL	0.063453	0.07031	0.1119	0.286762	0.0993166	0.099317	0.125118998	0.239525553	0.057929248	1.153642684	0.111911518	10.308525
AS	0.095179	0.14062	0.0373	0.095587	0.0993166	0.099317	0.250237997	0.079841851	0.115858496	1.013261477	0.095587175	10.60039144
TEMP	0.190358	0.14062	0.1119	0.095587	0.0993166	0.099317	0.125118998	0.079841851	0.057929248	1	0.099316599	10.06881032
WS	0.190358	0.14062	0.1119	0.095587	0.0993166	0.099317	0.125118998	0.079841851	0.057929248	1	0.099316599	10.06881032
PTR	0.063453	0.046873	0.1119	0.047794	0.0993166	0.099317	0.125118998	0.399209255	0.405504736	1.398497297	0.125118998	11.1773377
PTA	0.095179	0.046873	0.0373	0.095587	0.0993166	0.099317	0.0250238	0.079841851	0.231716992	0.810159223	0.079841851	10.14704962
PTU	0.063453	0.035155	0.1119	0.047794	0.0993166	0.099317	0.017874143	0.019960463	0.057929248	0.552709842	0.057929248	9.541118884

Note: FT fuel type, EL elevation, SL slope, AS aspect, TEMP temperature, WS wind speed, PTR proximity to road, PTA proximity to agriculture, PTU proximity to urban area, CW criteria weights**,** WSV weight sum value.

and reclassified on a scale from 1 (very low) to 5 (very high). These factors were then assigned weights using the AHP and integrated to generate the final map.

$$FS = \sum_{k=0}^{n} xi \times wi \quad (7)$$

where: *FS* is the fire susceptibility; *n* is the number of decision criteria; *xi* is the particular normalized criterion; *i* is the weight assigned to that criterion. These weighted values are then added together to create the final fire susceptibility output map.

Table 7. Random inconsistency values (Saaty, 1987)

n	2	3	4	5	6	7	8	9
RI	0	0.52	0.9	1.12	1.24	1.32	1.41	1.45

RESULTS AND DISCUSSION

The forest fire risk assessment in Lebanon was based on nine essential factors which are: elevation, slope, aspect, distance from urban areas, proximity to agricultural land, distance to roads, fuel types, temperature, wind speed and land use/land cover. By analyzing these factors, we were able to map and identify the areas most susceptible to fires. A detailed overview of each factor, including how they were classified and weighted in the assessment of fire risk zones, is provided below (Table 8)

Topography

Slope

The reclassified slope map (Figure 8) indicates that approximately 16.48% (176,000 ha) of the study area has slopes between 0 and 5 degrees, representing the lowest fire susceptibility. Around 18.22% (194,500 ha) of the area is classified as having low susceptibility (5–10°), while 50.5% (539,300 ha) falls into the moderate susceptibility range (10–20°). Areas with high (20–30°) and very high (>30°) fire susceptibility make up about 13.9% (148,500 ha) and 0.91% (9700 ha), respectively (Figure 5). It was found that forest fire incidents were most frequent on moderate and high slopes, with 1069 and 583 incidents respectively, and fewer occurrences on steeper slopes.

Aspect (Degree)

In the study area, slopes were classified into categories based on their aspect: very low (flat), low (northeast), moderate (northwest), high (east-southeast), and very high (southwest). These categories cover 0.19% (2000 ha), 1.46% (15,600 ha), 2.3% (24,500 ha), 41.61% (444,400 ha), and 54.44% (581,500 ha), respectively (Figure 8). It was found that forest fire incidents were most frequent in areas with very high and high aspects, with 1122 and 777 incidents respectively, and fewer occurrences in other directions (Figure 6).

Elevation

As shown in elevation map (Figure 8) areas with lower elevations, particularly those located along the western part of Lebanon where the altitude is below 500 meters above sea level, are the most vulnerable to fire risk. As elevation increases from the western part of the country towards the center, culminating in the Bekaa Valley where the highest elevations are found, the vulnerability to fire decreases, with 14.85% (158,600 ha) and 8.08% (86,300 ha) of the area exhibiting low and very low susceptibility to fire risk, respectively. Conversely, approximately 24.32% (259,800 ha) and 26.97% (288,000 ha) of the study area are classified as very high and high fire risk zones, respectively, corresponding to regions with elevations ranging from 0–500 meters and 500–1.000 meters, respectively. As the elevation continues to increase towards the Bekaa Valley, fire risk decreases further, with areas at 1000–1500 meters exhibiting moderate susceptibility, covering 25.78% (275,300 ha) of the region. It was observed that forest fire incidents were predominantly concentrated in the lowest elevation ranging from 0–500 meters and 500–1000 meters with 809 and 784 incidents respectively, with fewer occurrences at higher elevations and none in the highest areas of the study region (Figure 7). This pattern is likely attributed to the increased moisture content in vegetation and soil at these elevations, which diminishes the risk of fire ignition and spread

Metrological data

Temperature (C-degree)

Elevated temperatures accelerate evaporation, resulting in drier vegetation that is more susceptible to ignition and burns with greater intensity. The average monthly temperatures ranged from 13.3 °C to 41.2 °C, with maximum temperatures recorded during fire events falling between 23 °C and 41 °C.

The reclassified temperature map was classified into five categories: very low (T < 32°), low

Table 8. Classification and weight for different factors for assessment of forest fire risk zone

Thematic layers	Subclass	Divisions	Rate	Area (ha)	Area (%)
Topography	Elevation (m)	0–500	5	259,800	24.32
		500–1000	4	288,000	26.97
		1000–1500	3	275,300	25.78
		1500–2000	2	158,600	14.85
		2000–3033	1	86,300	8.08
	Slope (°)	0–5	1	176,000	16.48
		5–10	2	194,500	18.22
		10–20	3	539,300	50.5
		20–30	4	148,500	13.9
		30–80	5	9,700	0.9
	Aspect (°)	SW	5	581,500	54.44
		ES	4	444,400	41.61
		NW	3	24,500	2.3
		NE	2	15,600	1.46
		Flat	1	2,000	0.19
Anthropogenic factors	Proximity to roads (m)	0–100 m	5	487,100	45.61
		100–200 m	4	235,900	22.09
		200–300 m	3	112,600	10.54
		300–400 m	2	52,300	4.9
		> 400 m	1	180,100	16.86
	Proximity to urban (m)	0–100 m	5	261,085	24.49
		100–200 m	4	198,280	18.6
		200–300 m	3	123,125	11.55
		300– 400 m	2	78,215	7.33
		> 400 m	1	405,560	38.03
	Proximity to agriculture (m)	0–100 m	5	332,100	31.11
		100–200 m	4	213,900	20.04
		200–300 m	3	129,700	12.15
		300–400 m	2	82,100	7.7
		> 400 m	1	309,600	29
Climate	Temperature (°C)	T<32	1	531,200	38.78
		32<T<34	2	480,000	35.05
		34<T<36	3	76,800	5.61
		36<T<38	4	108,800	7.94
		T>38	5	172,800	12.62
	Wind speed (m/s)	W<2.8	1	134,525	13.11
		2.8<W<3.5	2	93,900	9.15
		3.5<W<4.4	3	279,425	27.23
		4.4<W<5.3	4	132,825	12.94
		W>5.3	5	385,600	37.57
Fuel types	Agriculture	Protected agriculture	1	230,171.25	35.6
		Fruit trees	1		
		Vineyards	1		
		Field crops in medium to large terrace	1		
		Field crops in small fields/terrace	1		
		Olives	3		
	Forest	Clear oaks	2	85,626.75	13.24
		Dense oaks	3	235,145.50	36.37
		Scrubland with some dispersed bigger trees	3		
		Clear grasslands	3		
		Dense-other types of broadleaved trees	4	28,634.75	4.43
		Clear-other types of broadleaved trees	4		
		Clear mixed wooded lands	4		

Table 8. Cont. Classification and weight for different factors for assessment of forest fire risk zone

Thematic layers	Subclass	Divisions	Rate	Area (ha)	Area (%)
Fuel types	Forest	Dense pines	5	67,010	10.36
		Dense mixed wooded lands	5		
		Burnt wooded lands	5		
		Clear fir	5		
		Clear pines	5		
		Dense fir	5		
		Dense cypress	5		
		Clear cedars	5		
		Clear juniper	5		

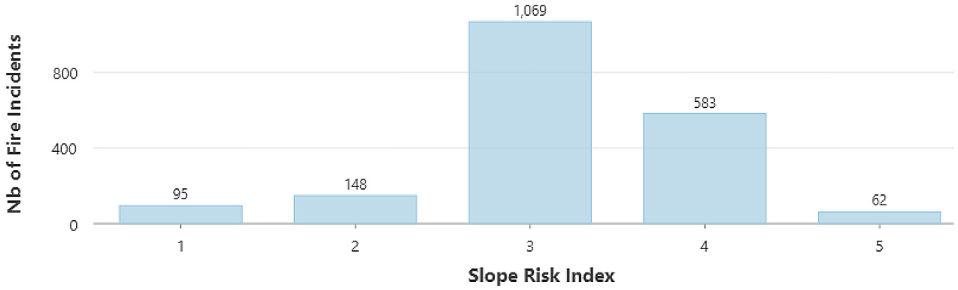

Figure 5. Frequency of fire incidents with respect to slope risk index

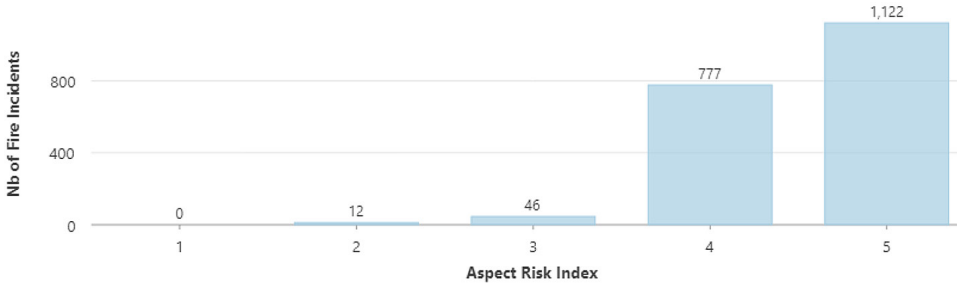

Figure 6. Frequency of fire incidents with respect to aspect risk index

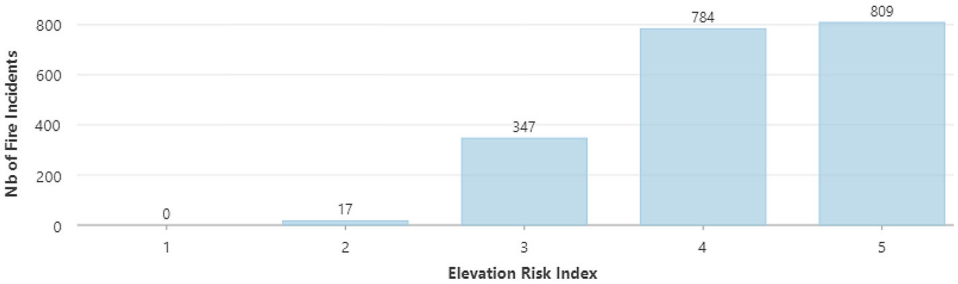

Figure 7. Frequency of fire incidents with respect to elevation risk index

(32° < T < 34°), moderate (34° < T < 36°), high (36° < T < 38°) and very high (T > 38°).

The areas with low temperature had very few fire occurrences due to the high moisture content in the fuel, which made the conditions less suitable for ignition of fire (Figure 8).

Wind speed

The reclassified wind speed map (Figure 8) shows that about 13.11% (134,525 ha) of the study area has an average wind speed < 2.8 m/s which belongs to lowest susceptibility to fire. About 9.15% (93,900 ha) and 27.23% (279,425 ha) of the

study area are characterized by low (2.8 < W < 3.5 m/s) and moderate (3.5 < W < 4.4 m/s) susceptibility to fire, respectively. Areas of high (4.4 < W < 5.3 m/s) and very high (W > 5.3 m/s) fire susceptibility cover about 12.94% (132,825 ha) and 37.57% (385,600 ha), respectively. The range of monthly average wind speeds recorded in the study area was between 1.11 and 12.5 meters per second.

Land use and land cover

Fuel types

In this study, LULC data obtained from CNRS has been categorized into two categories, forests and agriculture and the rate were assessed following the Lebanese NAP (2003). LULC was classified under 5 categories very low, low, moderate, high and very high with area covers 35.6% (230171.25 ha), 13.24% (85626.75 ha) 36.37% (235145.5 ha), 4.43% (28634.75 ha) and 10.36% (67010 ha) respectively (Figure 8). In our study, most fire incidents were observed in areas with moderate fire susceptibility.

Proximity to urban

In the study area, regions within 100 meters from urban areas are categorized as having very high susceptibility to fire, with a risk rating of 5. Areas within distances of 100 to 200 meters, 200 to 300 meters, and 300 to 400 meters are considered to have high, moderate, and low fire risk, with risk ratings of 4, 3, and 2, respectively. Areas located more than 400 meters away from urban regions are categorized as having very low fire risk, with a rating of 1 (Figure 8).

Proximity to agriculture

In the study area, locations within 100 meters of agricultural lands are categorized as having very high susceptibility to fire, with a risk rating of 5. Areas within 100 to 200 meters, 200 to 300 meters, and 300 to 400 meters are classified as having high, moderate, and low fire risk, with risk ratings of 4, 3, and 2, respectively. Areas more than 400 meters away from agricultural lands are categorized as having very low fire risk, with a rating of 1. It was found that forest fire incidents were more frequent in areas closest agriculture lands, with 597 and 477 incidents, respectively, and less frequent further away from the agriculture areas (Figure 8).

Proximity to roads

In the study area, regions within 100 meters from roads are categorized as having very high susceptibility to fire, with a risk rating of five. Areas within distances of 100–200 meters, 200–300 meters, and 300–400 meters are considered to have high, moderate, and low fire risk, with risk ratings of 4, 3, and 2, respectively. Areas located more than 400 meters away from roads are categorized as having very low fire risk, with a rating of 1. It was found that forest fire incidents were most frequent closest to roads, with 1059 and 651 incidents, respectively, and less frequent further away from the roads (Figure 8).

Stakeholder collaboration and implementation considerations

Active collaboration with various stakeholders is necessary for effective wildfire risk management. The initiative aims to enhance response capabilities, involving various stakeholders such as civil defense and community emergency response teams.

Additionally, following the community-based disaster risk reduction approach through training initiatives and awareness campaigns leads to more safe and resilient communities by raising preparedness to mitigate the risk of fire. Implementation efforts can be strengthened by collaborating with local organizations and NGOs through building capacities of existing structures within the communities. Also, applying this map NGOs may prioritize their target areas based on identified high risk zones where communities can benefit from several funded projects and activities related to this kind of hazard and other natural hazards.

FOREST FIRE RISK MAP OF THE STUDY AREA

The forest fire risk map was developed using geospatial technology and AHP. Final weights of all parameters were first determined. Then, the data was converted into raster format and combined with a raster calculator in ArcGIS to define the potential fire risk zones. The resulting scores were classified into five categories: very high (5), high (4), moderate (3), low (2), and very low (1).

Table 8 details the area distribution for each risk category: very low (4.5% or 39,650 ha), low

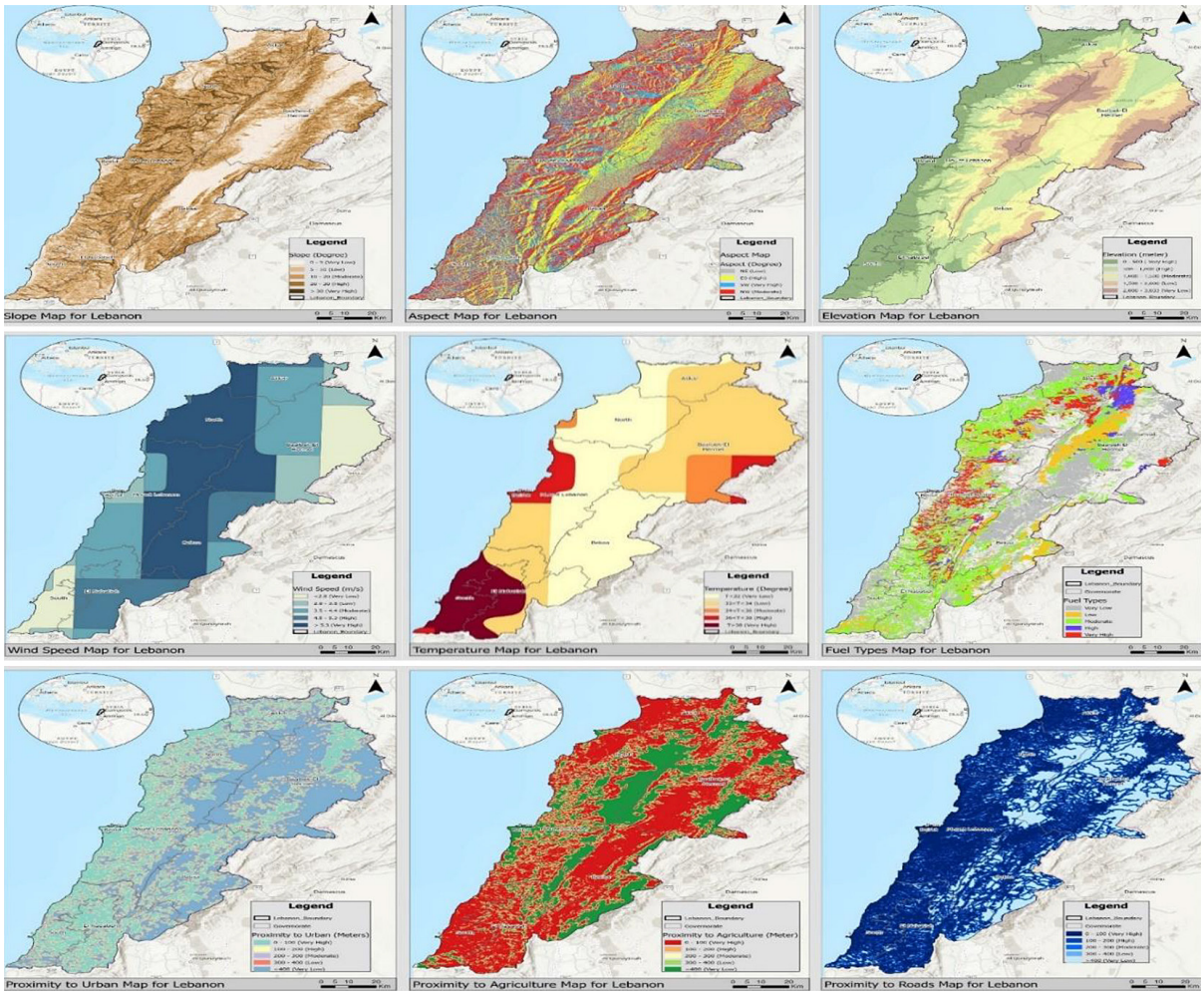

Figure 8. Reclassification of fire controlling factors

(19.54% or 172,425 ha), moderate (34.89% or 307,950 ha), high (33.45% or 295,225 ha), and very high (7.62% or 67,275 ha). The highest risk areas were mainly located in sparsely populated regions, especially in the western and southern parts of the district where agricultural and human activities are extensive. Moreover, areas of very high fire susceptibility were mostly found in lower elevation ranges with gentle slopes, particularly in the western part of the study area (Figure 9).

VALIDATION OF FIRE RISK ZONE MAP

To verify the accuracy of the fire risk zone map we should compare it with fire point data from the MODIS satellite. Fire polygons were placed over the risk zone map for the study area. Using the Spatial Analyst tool in GIS. The percentage of land with each risk zone was calculated based on the method outlined in Equation 8. The proportion of the area affected by fires was then computed using following equation:

$$Percentage\ of\ an\ area\ (\%) = \\ = \frac{estimated\ area}{total\ area} \times 100 \quad (8)$$

Validating the model is essential to ensure its predictions accurately reflect real-world conditions. This involves comparing the model's results with actual fire incidents. In this study, the validation was carried out by cross-referencing historical fire data from MODIS with the fire-prone areas indicated on the risk map.

The analysis of fire points detected by MODIS over the past 20 years confirmed the model's reliability (Table 9). The results revealed that fires were more common in low to moderate elevation areas, with a significant correlation between fire occurrences and the high-risk zones identified on the map.

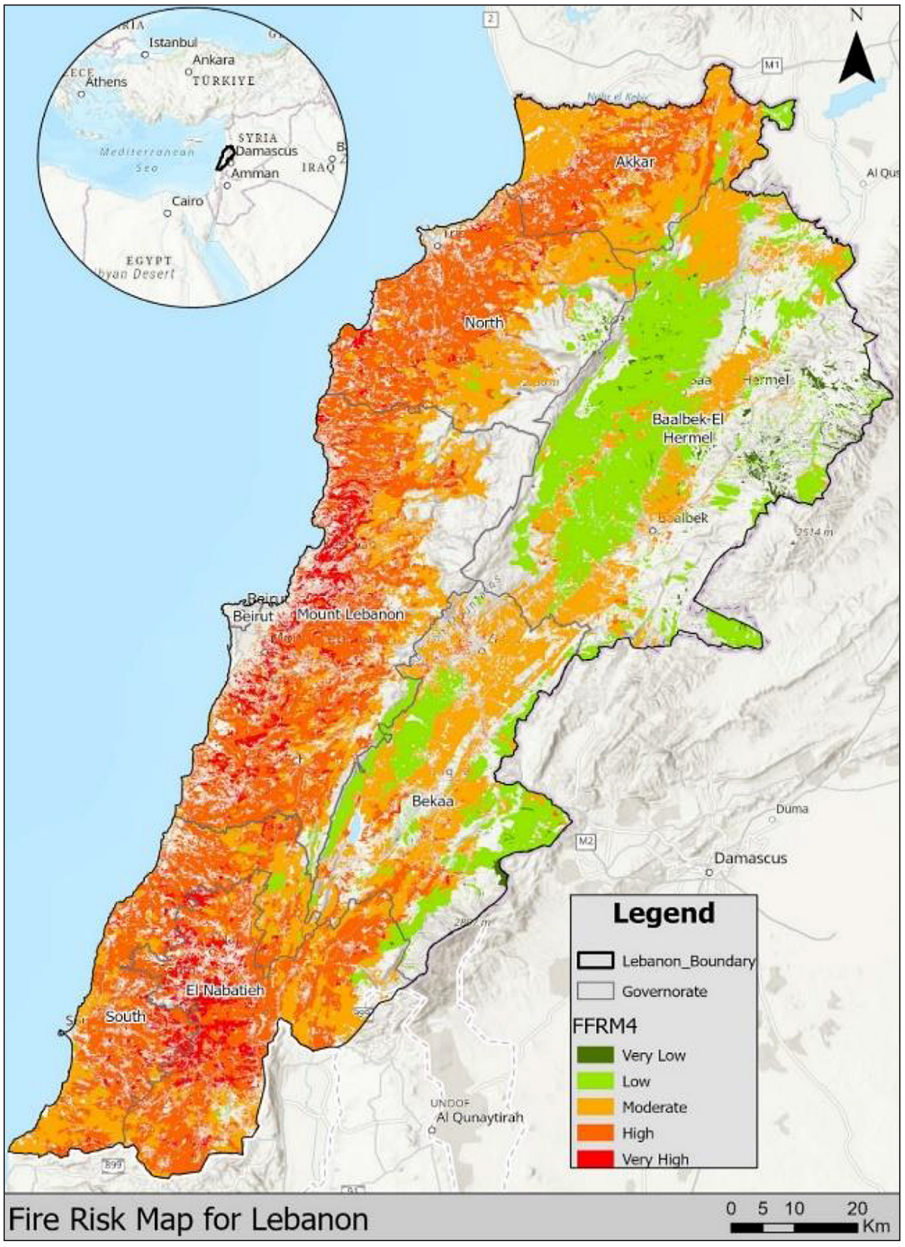

Figure 9. Fire susceptibility map of the study area

Table 9. Validation of Forest fire risk zones detected by the MODIS satellite over the past 20 years

Fire susceptibility	Area (ha)	Area (%)
Very low (1)	7.060284	0.06
Low (2)	766.828381	6.18
Moderate (3)	3069.998585	24.74
High (4)	7090.562629	57.15
Very high (5)	1472.134795	11.87

Additionally, data extracted from the Fire Incidents Dashboard related to the Lebanese Red Cross was overlaid on the fire risk model (FRM) to further assess its accuracy (Table 10). This data collection began in April 2024 and will continue to be updated on a weekly basis. Overlaying point data onto the output map is a technique for verifying the model's accuracy, a method that has been utilized in various studies (Hagos et al., 2022; Ogato et al., 2020). The

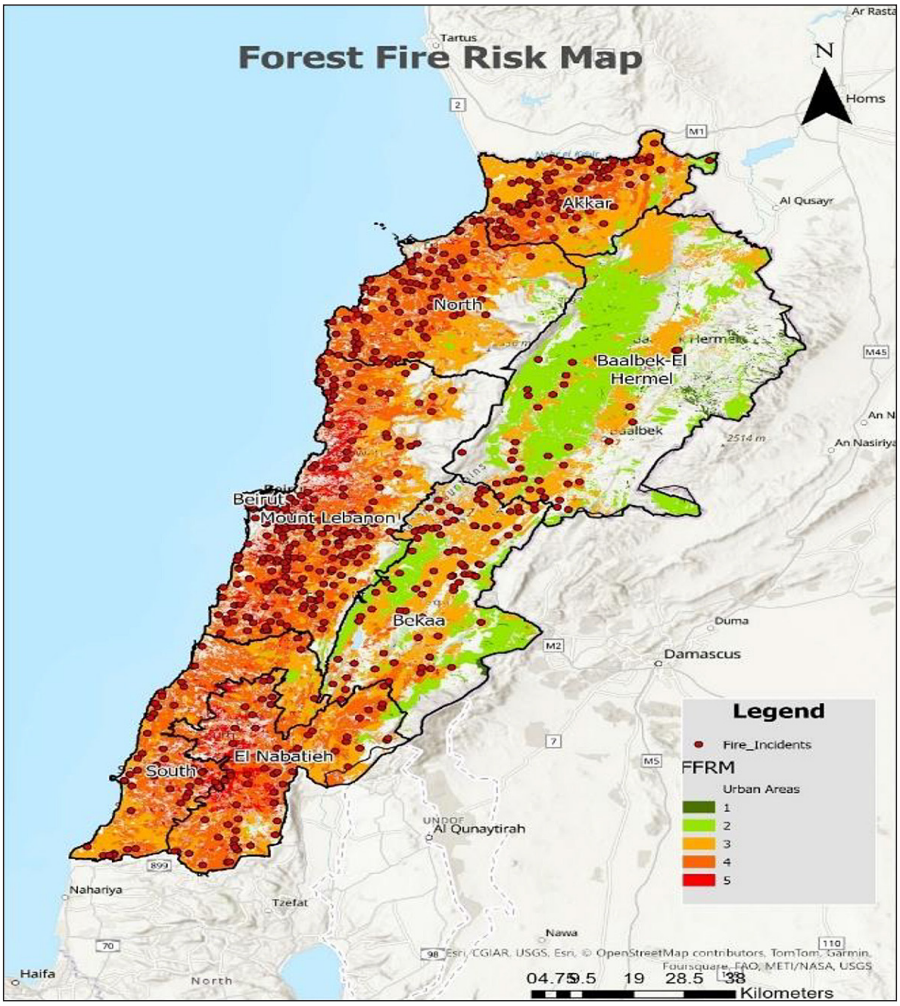

Figure 10. Validation map of the Fire susceptibility map

Table 10. Validation of fire incidents detected by the dashboard of the Lebanese Red Cross

Fire susceptibility	Number of incidents
Very low (1)	0
Low (2)	24
Moderate (3)	348
High (4)	1,111
Very high (5)	514

points correspond to the high-susceptibility areas identified by the model, indicating that the fire events recorded in the field align well with the FRM generated by the study (Figure 10).

CONCLUSIONS

This study investigates the use of geospatial technologies and the AHP to evaluate fire risk in Lebanon, taking into account factors such as elevation, slope, aspect, proximity to urban areas, agriculture, roads, temperature, wind speed, and fuel types. The fire risk map generated from this evaluation categorizes the area into five risk zones: very high, high, moderate, low, and very low. The analysis revealed that approximately 34.89% of the area had moderate fire risk, 33.45% was classified as high risk, and 7.62% was identified as very high risk. The remaining 19.54% showed low susceptibility, while 4.5% was in the very low risk category. The model's validity was confirmed through a comparison with historical fire data, showing a strong alignment between the model's predictions and actual fire events. The integration of GIS-based methods, AHP, and MCDM has proven effective in mapping fire-prone areas, highlighting its utility for fire risk management showing the total area burned (mapping), the seasonal timing of flames, and the exact locations of fire boundaries. These

findings provide valuable insights for local authorities in planning for large-scale fire hazards and suggest that the methodology can be adapted for other regions within the Mediterranean basin facing similar fire risks. The produced risk map also improves safety procedures, such as resource allocation and creation of evacuation plans during fire events. Besides, it can help guide strategic decision-making directing initiatives and fire control measures. Thus, can develop a comprehensive and proactive framework for managing wildfires at the local and national levels.

Acknowledgment

The authors would like to acknowledge the Lebanese Red Cross Disaster Risk Reduction (DRR) unit for providing essential data and the Lebanese University for their support and resources.

REFERENCES

1. Abdo, H. G., Almohamad, H., Al Dughairi, A. A., & Al-Mutiry, M. (2022). GIS-based frequency ratio and analytic hierarchy process for forest fire susceptibility mapping in the western region of Syria. *Sustainability, 14*(8), 4668. https://doi.org/10.3390/su14084668
2. Abu Dabous, S., & Alkass, S. (2008). Decision support method for multi-criteria selection of bridge rehabilitation strategy. *Construction Management and Economics, 26*(8), 883–893. https://doi.org/10.1080/01446190802213537
3. Agarwal, C. (2002). A review and assessment of land-use change models: Dynamics of space, time, and human choice. [Publisher and DOI information not available].
4. Aini, A., Curt, T., & Bekdouche, F. (2019). Modelling fire hazard in the southern Mediterranean fire rim (Bejaia region, northern Algeria). *Environmental Monitoring and Assessment, 191*(12), 747. https://doi.org/10.1007/s10661-019-7834-0
5. Alexandrian, D., Esnault, F., & Calabri, G. (1999). Forest fires in the Mediterranean area. [Publisher or report details not available; DOI unavailable].
6. Belhadj-Khedher, C., Koutsias, N., Karamitsou, A., EI-Melki, T., Ouelhazi, B., Hamdi, A.,... & Mouillot, F. (2018). A revised historical fire regime analysis in Tunisia (1985–2010) from a critical analysis of the national fire database and remote sensing. *Forests, 9*(2), 59. https://doi.org/10.3390/f9020059
7. Bellman, R. E., & Zadeh, L. A. (1970). Decision-making in a fuzzy environment. *Management Science, 17*(4), B-141. https://doi.org/10.1287/mnsc.17.4.B141
8. Bugh, G. R., Kingston, P., Barnett, R. D., Khalaf, S. G., Maksoud, C. F., & Ochsenwald, W. L. (2024, August 26). Lebanon. *Encyclopedia Britannica*. Retrieved from https://www.britannica.com/place/Lebanon
9. Bui, D. T., Van Le, H., & Hoang, N. D. (2018). GIS-based spatial prediction of tropical forest fire danger using a new hybrid machine learning method. *Ecological Informatics, 48*, 104–116. https://doi.org/10.1016/j.ecoinf.2018.08.007
10. Chen, S. J., & Hwang, C. L. (1992). Fuzzy multiple attribute decision-making methods. In *Fuzzy multiple attribute decision making: Methods and applications* 289–486. Berlin, Heidelberg: Springer. https://doi.org/10.1007/978-3-642-46768-4_7
11. CNRS-L. (2019). *Land cover/land use map of Lebanon* (Scale 1:20.000). Centre National de la Recherche Scientifique-Liban (CNRS-L).
12. Convention on Biological Diversity. (n.d.). Country profile: Lebanon. Retrieved from https://www.cbd.int/countries/profile?country=lb
13. Danumah, J. H., Odai, S. N., Saley, B. M., Szarzynski, J., Thiel, M., Kwaku, A.,... & Akpa, L. Y. (2016). Flood risk assessment and mapping in Abidjan district using multi-criteria analysis (AHP) model and geoinformation techniques (Côte d'Ivoire). *Geoenvironmental Disasters, 3*(1), 1–13. https://doi.org/10.1186/s40677-016-0044-x
14. Dimitrakopoulos, A. P., & Mitsopoulos, I. D. (2006). Global forest resources assessment 2005: Report on fires in the Mediterranean region. *Fire Management Working Papers (FAO), 8*.
15. El Hafyani, M., Essahlaoui, A., Van Rompaey, A., Mohajane, M., El Hmaidi, A., El Ouali, A.,... & Serrhini, N. E. (2020). Assessing regional-scale water balances through remote sensing techniques: A case study of Boufakrane River Watershed, Meknes Region, Morocco. *Water, 12*(2), 320. https://doi.org/10.3390/w12020320
16. Esri. (n.d.). How aspect works. Retrieved August 26, 2024, from https://pro.arcgis.com/en/pro-app/latest/tool-reference/spatial-analyst/how-aspect-works.htm
17. Faour, G. (2004). Forest fire fighting in Lebanon using remote sensing and GIS. *Technical Report*.
18. Faour, G., Kheir, R. B., & Verdeil, É. (2006). Caractérisation sous système d'information géographique des incendies de forêts: l'exemple du Liban. *Forêt Méditerranéenne, 27*(4), 339–352.
19. Faour, G. (2015). Evaluating urban expansion using remotely-sensed data in Lebanon. *Lebanon Science Journal, 16*, 23–32.
20. Ghali, R., Jmal, M., Souidene Mseddi, W., & Attia, R. (2020). Recent advances in fire detection and monitoring systems: A review. In *Proceedings of*

the 8th International Conference on Sciences of Electronics, Technologies of Information and Telecommunications (SETIT'18), Vol. 1 (pp. 332–340). Springer International Publishing. https://doi.org/10.1007/978-3-030-21012-6_36

21. Giglio, L., Schroeder, W., & Justice, C. O. (2016). The collection 6 MODIS active fire detection algorithm and fire products. *Remote Sensing of Environment, 178*, 31–41. https://doi.org/10.1016/j.rse.2016.02.054
22. Gill, A. M. (1975). Fire and the Australian flora: A review. *Australian Forestry, 38*(1), 4–25. https://doi.org/10.1080/00049158.1975.10675685
23. Gill, A. M., Stephens, S. L., & Cary, G. J. (2013). The worldwide "wildfire" problem. *Ecological Applications, 23*(2), 438–454. https://doi.org/10.1890/10-2213.1
24. Global Forest Watch. (2024). Lebanon fires dashboard. Retrieved July 30, 2024, from https://www.globalforestwatch.org/dashboards/country/LBN/?category=fires
25. Hagos, Y. G., Andualem, T. G., Yibeltal, M., & Mengie, M. A. (2022). Flood hazard assessment and mapping using GIS integrated with multi-criteria decision analysis in upper Awash River basin, Ethiopia. *Applied Water Science, 12*(7), 148. https://doi.org/10.1007/s13201-022-01665-3
26. Jain, P., Coogan, S. C., Subramanian, S. G., Crowley, M., Taylor, S., & Flannigan, M. D. (2020). A review of machine learning applications in wildfire science and management. *Environmental Reviews, 28*(4), 478–505. https://doi.org/10.1139/er-2020-0019
27. Key, C. H., & Benson, N. C. (1999). The Normalized Burn Ratio (NBR): A Landsat TM radiometric measure of burn severity. *United States Geological Survey, Northern Rocky Mountain Science Center*.
28. Kumar, M., Denis, D. M., Singh, S. K., Szabó, S., & Suryavanshi, S. (2018). Landscape metrics for assessment of land cover change and fragmentation of a heterogeneous watershed. *Remote Sensing Applications: Society and Environment, 10*, 224–233. https://doi.org/10.1016/j.rsase.2018.02.002
29. Vadrevu, K. P., Eaturu, A., & Badarinath, K. (2010). Fire risk evaluation using multicriteria analysis—a case study. *Environmental Monitoring and Assessment, 166*, 223–239. https://doi.org/10.1007/s10661-009-0997-6
30. Lamat, R., Kumar, M., Kundu, A., & Lal, D. (2021). Forest fire risk mapping using analytical hierarchy process (AHP) and earth observation datasets: A case study in the mountainous terrain of Northeast India. *SN Applied Sciences, 3*(4), 425. https://doi.org/10.1007/s42452-021-04431-5
31. Majdalani, G., Koutsias, N., Faour, G., Adjizian-Gerard, J., & Mouillot, F. (2022). Fire regime analysis in Lebanon (2001–2020): Combining remote sensing data in a scarcely documented area. *Fire, 5*(5), 141. https://doi.org/10.3390/fire5050141
32. Majlingová, A. (2015). Automated procedure to assess the susceptibility of forest to fire. *Journal of Forest Science, 61*(6), 255–260. https://doi.org/10.17221/13/2015-JFS
33. Masri, T., Khawlie, M., Faour, G., & Awad, M. (2003, June). Mapping forest fire prone areas in Lebanon. In *Proceedings of the EARSeL 23rd Symposium of Remote Sensing in Transition – 4th International Workshop on Remote Sensing and GIS Applications to Forest Fire Management* (pp. 109–113).
34. Mazzeo, G., De Santis, F., Falconieri, A., Filizzola, C., Lacava, T., Lanorte, A.,... & Satriano, V. (2022). Integrated satellite system for fire detection and prioritization. *Remote Sensing, 14*(2), 335. https://doi.org/10.3390/rs14020335
35. Ministry of Environment, Lebanon. (2024). Vulnerability and adaptation. Retrieved July 30, 2024, from https://climatechange.moe.gov.lb/vulnerability-and-adaptation
36. Mittermeier, R. (2005). *Hotspots revisited: Earth's biologically richest and most endangered terrestrial ecoregions*.
37. MoE-UNDP-UNICEF-UNHCR (United Nations High Commission for Refugees). (2020). *Lebanon State of the Environment and Future Outlook: Turning the Crises into Opportunities.*
38. Mohajane, M., Costache, R., Karimi, F., Pham, Q. B., Essahlaoui, A., Nguyen, H.,... & Oudija, F. (2021). Application of remote sensing and machine learning algorithms for forest fire mapping in a Mediterranean area. *Ecological Indicators, 129*, 107869. https://doi.org/10.1016/j.ecolind.2021.107869
39. NASA FIRMS. (n.d.). FIRMS: Fire Information for Resource Management System. NASA. Retrieved August 26, 2024, from https://firms.modaps.eosdis.nasa.gov/
40. NASA. (n.d.). ASTER Global Digital Elevation Model (GDEM). *NASA Earthdata.* Retrieved from https://earthdata.nasa.gov
41. Ogato, G. S., Bantider, A., Abebe, K., & Geneletti, D. (2020). Geographic information system (GIS)-based multicriteria analysis of flooding hazard and risk in Ambo Town and its watershed, West Shoa Zone, Oromia Regional State, Ethiopia. *Journal of Hydrology: Regional Studies, 27,* 100659. https://doi.org/10.1016/j.ejrh.2019.100659
42. Paula, S., Arianoutsou, M., Kazanis, D., Tavsanoglu, Ç., Lloret, F., Buhk, C.,... & Pausas, J. G. (2009). Fire-related traits for plant species of the Mediterranean Basin: Ecological Archives E090-094. *Ecology, 90*(5), 1420. https://doi.org/10.1890/08-1309.1
43. Pinto, M. M., Trigo, R. M., Trigo, I. F., & DaCamara, C. C. (2021). A practical method for high-resolution

burned area monitoring using Sentinel-2 and VIIRS. *Remote Sensing, 13*(9), 1608. https://doi.org/10.3390/rs13091608

44. Pourghasemi, H. R., Beheshtirad, M., & Pradhan, B. (2016). A comparative assessment of prediction capabilities of modified analytical hierarchy process (M-AHP) and Mamdani fuzzy logic models using Netcad-GIS for forest fire susceptibility mapping. *Geomatics, Natural Hazards and Risk, 7*(2), 861–885. https://doi.org/10.1080/19475705.2014.984247
45. PreventionWeb. (2022, September 15). Lebanon's forests: Dousing fire risks through stronger forest management. Retrieved July 30, 2024, from https://www.preventionweb.net/news/lebanons-forests-dousing-fire-risks-through-stronger-forest-management
46. Raval, P., & Motiani, R. (2022, August). Review of fire risk factors for fire risk assessment in urban areas: The case of Ahmedabad, India. In *International Conference on Innovation in Smart and Sustainable Infrastructure* (pp. 607–623). Singapore: Springer Nature Singapore.
47. Rothermel, R. C. (1983). *How to predict the spread and intensity of forest and range fires* (Vol. 143). U.S. Department of Agriculture, Forest Service, Intermountain Forest and Range Experiment Station.
48. Rouse Jr, J. W., Haas, R. H., Schell, J. A., & Deering, D. W. (1973). Monitoring the vernal advancement and retrogradation (green wave effect) of natural vegetation (No. NASA-CR-132982).
49. Ruffault, J., & Mouillot, F. (2015). How a new fire-suppression policy can abruptly reshape the fire-weather relationship. *Ecosphere, 6*(10), 1–19. https://doi.org/10.1890/ES15-00258.1
50. Ruffault, J., Curt, T., Moron, V., Trigo, R. M., Mouillot, F., Koutsias, N.,... & Belhadj-Khedher, C. (2020). Increased likelihood of heat-induced large wildfires in the Mediterranean Basin. *Scientific Reports, 10*(1), 13790. https://doi.org/10.1038/s41598-020-70779-3
51. Saaty, T. L. (1980). *The analytic hierarchy process (AHP). The Journal of the Operational Research Society, 41*(11), 1073–1076.
52. Sharma, N. R., Fernandes, P. J. F., & Pokarel, J. R. (2014). Methodological development for forest fire hazard in Nepal. *Revista Brasileira de Cartografia, 66*(7), 1551–1566.
53. Station. Mukherjee, S., & Raj, K. (2014). Analysis of forest fire of Meghalaya using geospatial tools. In *15th ESRI India User Conference 2014.* Retrieved from https://www.esri.in/
54. Szpakowski, D.M., & Jensen, J.L. (2019). A review of the applications of remote sensing in fire ecology. *Remote Sensing, 11*(22), 2638. https://doi.org/10.3390/rs11222638
55. Teodoro, A. C., & Duarte, L. (2013). Forest fire risk maps: A GIS open source application—a case study in Norwest of Portugal. *International Journal of Geographical Information Science, 27*(4), 699–720. https://doi.org/10.1080/13658816.2012.707613
56. Triantaphyllou, E., & Triantaphyllou, E. (2000). *Multi-criteria decision making methods* (pp. 5–21). Springer US.
57. Venkatesh, K., Preethi, K., & Ramesh, H. (2020). Evaluating the effects of forest fire on water balance using fire susceptibility maps. *Ecological Indicators, 110,* 105856. https://doi.org/10.1016/j.ecolind.2019.105856
58. Weatherbit. (n.d.). Weatherbit API documentation. Retrieved from https://www.weatherbit.io/api
59. World Bank. (2022a). Climate Change Knowledge Portal: Lebanon. Retrieved from https://climateknowledgeportal.worldbank.org/country/lebanon/climate-data-historical
60. World Bank. (2011). *Gray matters: Enhancing the quality of education and training in developing countries.* Washington, DC: World Bank.
61. https://documents1.worldbank.org/curated/en/360011468265768992/pdf/622660ESW0Gray0c060601100BOX361480B.pdf